Supporting Information

External forcing explains recent decadal variability of the ocean carbon sink

Galen A. McKinley[1], Amanda R. Fay[1], Yassir A. Eddebbar[2], Lucas Gloege[1],
Nicole S. Lovenduski[3]

[1] Lamont Doherty Earth Observatory / Columbia University, Palisades NY
[2] Scripps Institution of Oceanography, La Jolla, CA
[3] University of Colorado at Boulder, Boulder, CO

Models and Products

In addition to the 6 hindcast models used throughout this analysis, nine (9) hindcast model-based estimates of the effect of constant climate and variable $pCO_2^{atmosphere}$ for 1980-2016 are used to provide a comparison to other recent work (Devries et al. 2019; Figure 1b). Of the 9 models in this suite, 6 are essentially the same as those in our primary analysis. Correlation of the mean of this 9-member ensemble with variable climate and variable $pCO_2^{atmosphere}$ for 1980-2016 (Devries et al. 2019) to our suite of hindcast models is 0.99, indicating that the results are interchangeable for the purpose of this paper.

Flux analysis

Individual models and products utilize different methods for flux calculation including wind speed products and parameterizations. References included in Table S1 and Table S2 provide details on each model and product.

pCO_2 analysis

For both models and products, maps of flux indicate that ice coverage has been considered in the calculation, however spatially-resolved pCO_2 do not indicate this masking. Therefore, we begin by accounting for ice coverage in the pCO_2 analysis for each model and product [$pCO_2^{ocean} = pCO_2^{ocean,\,raw}$ *(1-ice fraction)] with ice fraction product NOAA_OI_SST_V2. These data provided by the NOAA/OAR/ESRL PSD, Boulder, Colorado USA from their website at https://www.esrl.noaa.gov/psd/ (Reynolds et al., 2002). The ice fraction product begins in 1982. In order to apply it to models that begin in 1980, we use the 1982-1989 monthly climatology for 1980 and 1981.

ΔpCO_2 is calculated at annual timescales by [$\Delta pCO_2 = pCO_2^{ocean} - pCO_2^{atmosphere}$] where $pCO_2^{atmosphere}$ is the dry air mixing ratio of atmospheric CO_2 (xCO_2) from the ESRL surface marine boundary layer CO_2 product available at https://www.esrl.noaa.gov/gmd/ccgg/mbl/data.php (Dlugokencky et al., 2017) multiplied by sea level pressure (Kalnay et al., 1996) at monthly resolution, taking into account the water vapor correction according to Dickson et al. (2007). NCEP Reanalysis Derived data provided by the NOAA/OAR/ESRL PSD, Boulder, Colorado, USA, from their web site at https://www.esrl.noaa.gov/psd/. A global area-weighted annual time series is then calculated for $pCO_2^{atmosphere}$ before calculating ΔpCO_2 for each model and product. Only the CNRM model accounted for water vapor pressure at the time it was run. For pCO_2 to be plotted consistently with CNRM and the observationally based products, we must apply an adjustment to the remaining models that do not include the water vapor correction. To do so, we offset their global mean pCO_2 time series by the difference between the observed $pCO_2^{atmosphere}$ calculated with and without the water vapor correction. This correction averages 9.2 µatm over years 1980-2017.

Upper Ocean Box Model, Additional Discussion

For the box model, the temperature is set at 14C, consistent with the observed SST global mean outside 15S-15N. The piston velocity of k_w = 25 cm/hr is higher than the global mean of

approximately 17 cm/hr (Wanninkhof, 2014; Neagler et al. 2006). This choice is justified by the lack of spatial variability in ΔpCO_2 and in piston velocity, normally parameterized as a square function of windspeed (Wanninkhof, 2014). Larger ΔpCO_2 are coincident at higher latitudes with stronger winds, and thus with larger piston velocities (Takahashi et al. 2009). Since the product of the global mean will naturally be less than the mean of the product when extreme values are correlated, a higher piston velocity is selected to allow for a reasonable ΔpCO_2 and air-sea CO_2 flux to co-exist in the box model.

The mean and standard deviation of the air-sea CO_2 flux in the box model is not very sensitive to reasonable parameter choices. Across the observed k_w range of 15-30 cm/hr (Wanninkhof, 2014), and reasonable estimates for the rate of overturning circulation (ν) from 40-80 Sv (DeVries et al., 2017), the mean flux is not sensitive, only varying by 0.5PgC/yr (Fig S3a). The depth of the box does impact the mean flux (Fig S3b,c) because these alter the volume and rate of supply of low carbon water from depth that must equilibrate with rising $pCO_2^{atmosphere}$. The magnitude of variability ranges by approximately 20% across k_w values, but is not sensitive to ν (Fig S3d). This sensitivity analysis indicates that our parameter choices do not dramatically influence our key result with respect to the magnitude and pattern of variability. In addition, our choice of parameters is supported by the fact that the box model forced with only $pCO_2^{atmosphere}$ can capture air-sea CO_2 flux variability that is essentially identical to the ensemble result from constant climate three-dimensional ocean models (Fig. 1b).

When the box model is forced with only the 1980-2017 linear change of $pCO_2^{atmosphere}$ (1.70 μatm/yr) (Fig S6a,d), there is a steadily growing carbon flux into the ocean in response to the growing $pCO_2^{atmosphere}$ (Fig S6e). The continued irrigation of the near-surface ocean with low DIC waters allows for continued growth of ΔpCO_2, consistent with the global long-term increasingly negative ΔpCO_2 (Fig. 2, McKinley et al. 2017). Because there are no short-term anomalies in either pCO_2^{ocean} or $pCO_2^{atmosphere}$ when forced with linear trend of $pCO_2^{atmosphere}$, there is also no interannual variability of ΔpCO_2 (Fig S6f) or flux (Fig S6h) in this case. Adding the volcano SST forcing (Fig S2) to the box model forced with linear $pCO_2^{atmosphere}$, there are immediate negative anomalies in ΔpCO_2, indicating an increased sink, and then a relaxation as the surface ocean re-warms with the fading of the volcano cooling effect (Fig S6e,f).

Table S1: Hindcast model resolution and coverage period. Total ocean coverage is based on the 1°x1° mask of Gruber et al., 2009 used in the RECCAP project (Canadell et al., 2011).

Model Name ***Reference***	**Resolution** **Years**	**Area Coverage** **(% global ocean)**
MITgcm-REcoM2 *Hauck et al. 2018*	Monthly, 1°x1° 1958-2017	3.51e+14m^2 (96%)
NEMO-PlankTOM *Buitenhuis et al. 2010*	Monthly, 1°x1° 1959-2017	3.49e+14m^2 (96%)
CNRM-ESM2-1 *Séférian et al. 2016*	Monthly, 1°x1° 1848-2017	3.61e+14 m^2 (99%)
CCSM-BEC *Doney et al. 2009*	Monthly, 1°x1° 1958-2017	3.29e+14m^2 (90%)
MPI-ESM *Paulsen et al. 2017*	Monthly, 1°x1° 1959-2017	3.42e+14m^2 (94%)
NorESM-OCv1.2 *Schwinger et al. 2016*	Monthly, 1°x1° 1948-2017	3.70e+14m^2 (101%)

Table S2: Observationally-based product resolution and coverage period. In the case of time-varying coverage masks, area coverage listed is for a most conservative mask which requires a value for every month of the time period. In some cases, this differs for flux and pCO_2 variables. Total ocean coverage is based on the 1x1° mask of Gruber et al., 2009 used in the RECCAP project (Canadell et al., 2011).

Product Name ***Reference***	**Resolution Years**	**Area Coverage (% global ocean)**	**Mean Correction to Flux (to pCO_2)** (section 2.4)
LSCE *Denvil-Sommer et al. 2019*	Monthly, 1°x1° 1985-2016	2.93e+14m^2 (80%)	0.41 $PgCyr^{-1}$ (3.16µatm)
CSIR-ML6 *Gregor et al. 2019*	Monthly, 1°x1° 1982-2016	Flux: 3.11e+14m^2 (85%) pCO_2: 3.13e+14 (86%)	0.33 $PgCyr^{-1}$ (2.46µatm)
SOM-FFN *Landschützer et al. 2017*	Monthly, 1°x1° 1982-2018	3.19e+14m^2 (87%)	0.25 $PgCyr^{-1}$ (1.55µatm)
Jena-MLS *Rödenbeck et al. 2013*	Monthly, 5°x5° 1982-2018 flux	3.67e+14m^2 (100%)	0

Table S3: Parameters and values for the upper ocean diagnostic box model

Parameter	Value	References / Notes
ν	60 Sv	Devries et al. 2017
DIC_{deep}	2055 mmol/m^3	Sarmiento and Gruber, 2006
k_w	25 cm/hr	Wanninkhof, 2014
Temperature	14^{o}C	
Salinity	35psu	
Alkalinity	2350 mmol/m^3	Sarmiento and Gruber, 2006
dz	200m	
Global ocean area (A)	3.34e14 m^2	96% of global ocean

Table S4: Correlation of air-sea carbon flux for hindcast models, observationally-based products, and box model runs as shown in Figure 1. Detrended timeseries correlations shown in parenthesis. Correlations are shown for longest overlapping timeseries. Correlations in bold are significant at $p<0.05$.

	Hindcast models 1980-2017	Box Model 1980-2017	Hindcast models: pCO_2^{atm} only 1980-2016	Box Model: pCO_2^{atm} only 1980-2017	OCIM: pCO_2^{atm} only 1980-2017
Observationally-based products 1985-2016	**0.95 (0.78)**	**0.89 (0.54)**	**0.86** (0.15)	**0.82** (0.17)	**0.87** (0.24)
Hindcast models 1980-2017	**1**	**0.92 (0.57)**	**0.89** (-0.01)	**0.86** (0.02)	**0.90** (-0.01)
Box Model 1980-2017	**-**	**1**	**0.91 (0.49)**	**0.89 (0.41)**	**0.91 (0.50)**
Hindcast models: pCO_2^{atm} only 1980-2016	**-**	**-**	**1**	**0.974)**	**0.99 (0.96)**
Box Model: pCO_2^{atm} only 1980-2017	**-**	**-**	**-**	**1**	**0.98 (0.91)**

Table S5: Global Mean Fluxes (PgC/yr) by decade. Observationally-based products have been masked to account for missing ocean area.

Global Mean Flux (PgC/yr)	1980-1989	1990-1999	2000-2009	2010-2017
Box Model: actual pCO_2^{atm} and volcano	-1.73	-1.86	-2.11	-2.43
Box Model: actual pCO_2^{atm}	-1.71	-1.82	-2.15	-2.43
Box Model: volcano only	-1.84	-2.03	-2.11	-2.20
Box Model: linear pCO_2^{atm}	-1.82	-1.99	-2. 15	-2.28
Hindcast model mean	-1.68	-1.90	-2.05	-2.37
Observationally-based product mean[a]	-1.87[b]	-2.07	-2.24	-2.86[c]

a. The mean flux of the observationally-based products is increased by 0.45 PgC/yr (Jacobson et al. 2007) to account for background outgassing of riverine carbon.
b. 3 observationally-based products begin in 1982 and 1 in 1985 (Table S2)
c. Observationally-based products through 2016 only

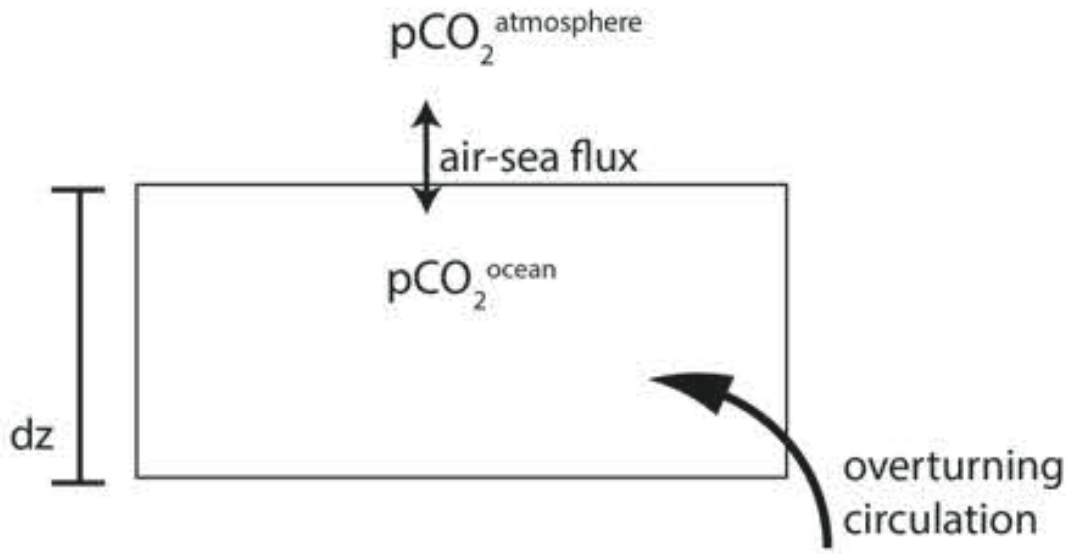

Figure S1: Schematic of the single-reservoir upper ocean diagnostic box model

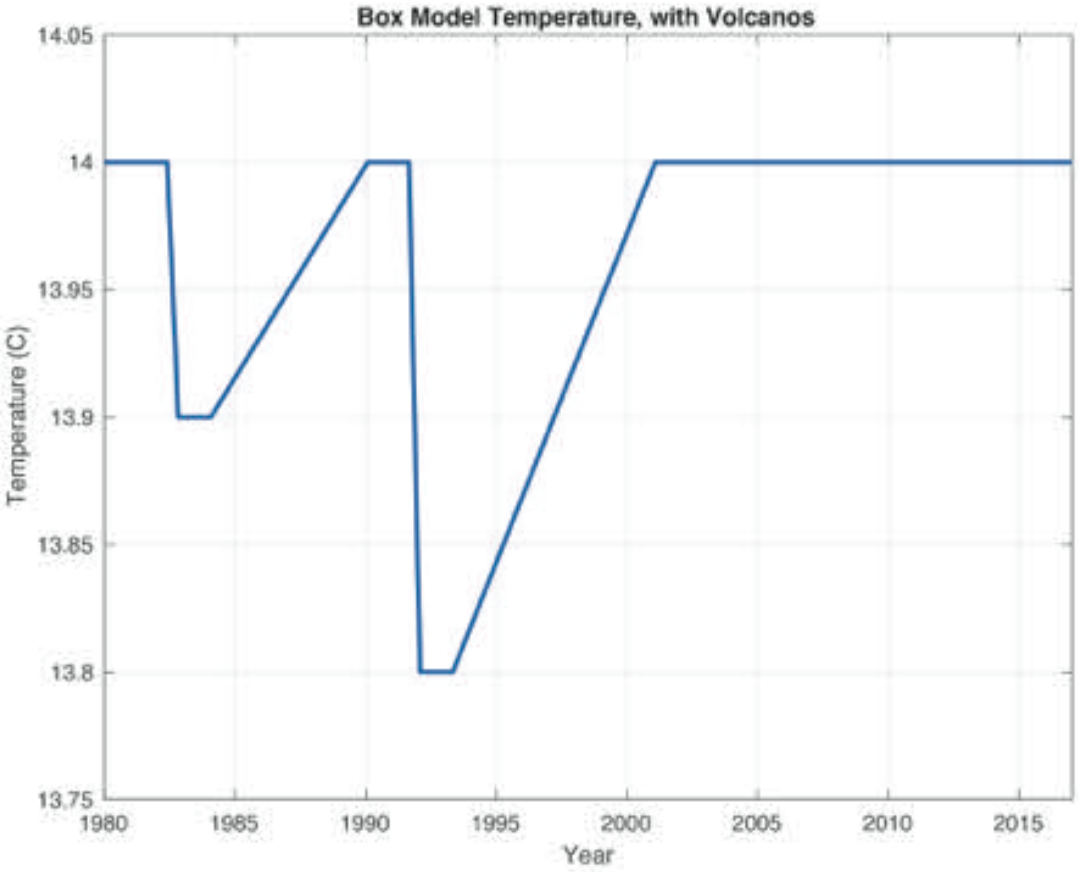

Figure S2: Sea surface temperature forcing for box model. Idealized SST response, based on two earth system models forced response to El Chichon and Mt. Pinatubo (Eddebbar et al. 2019, their Figure 1a)

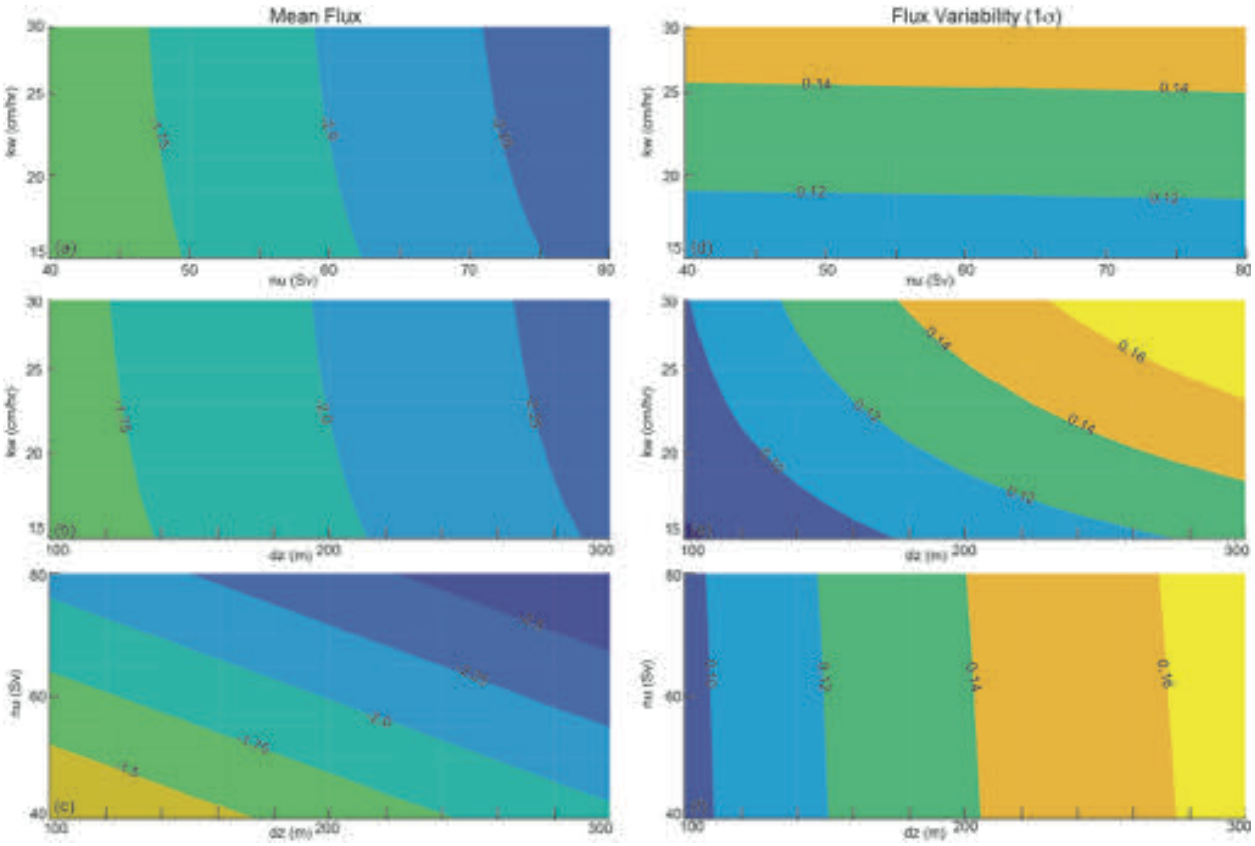

Figure S3: Sensitivity of the air-sea flux (PgC/yr) on the mean (a-c) and for variability (d-f) in the box model. The impact of varying values of piston velocity (k_w), the rate of the overturning circulation (ν), and the depth of the box (dz) on the box model forced with both $pCO_2^{atmosphere}$ and the SST response to volcanos. Default values are used for the third parameter in each case, e.g. (a,d) dz = 200m; (b,e), ν = 60 Sv; (c,f) k_w = 25 cm/hr.

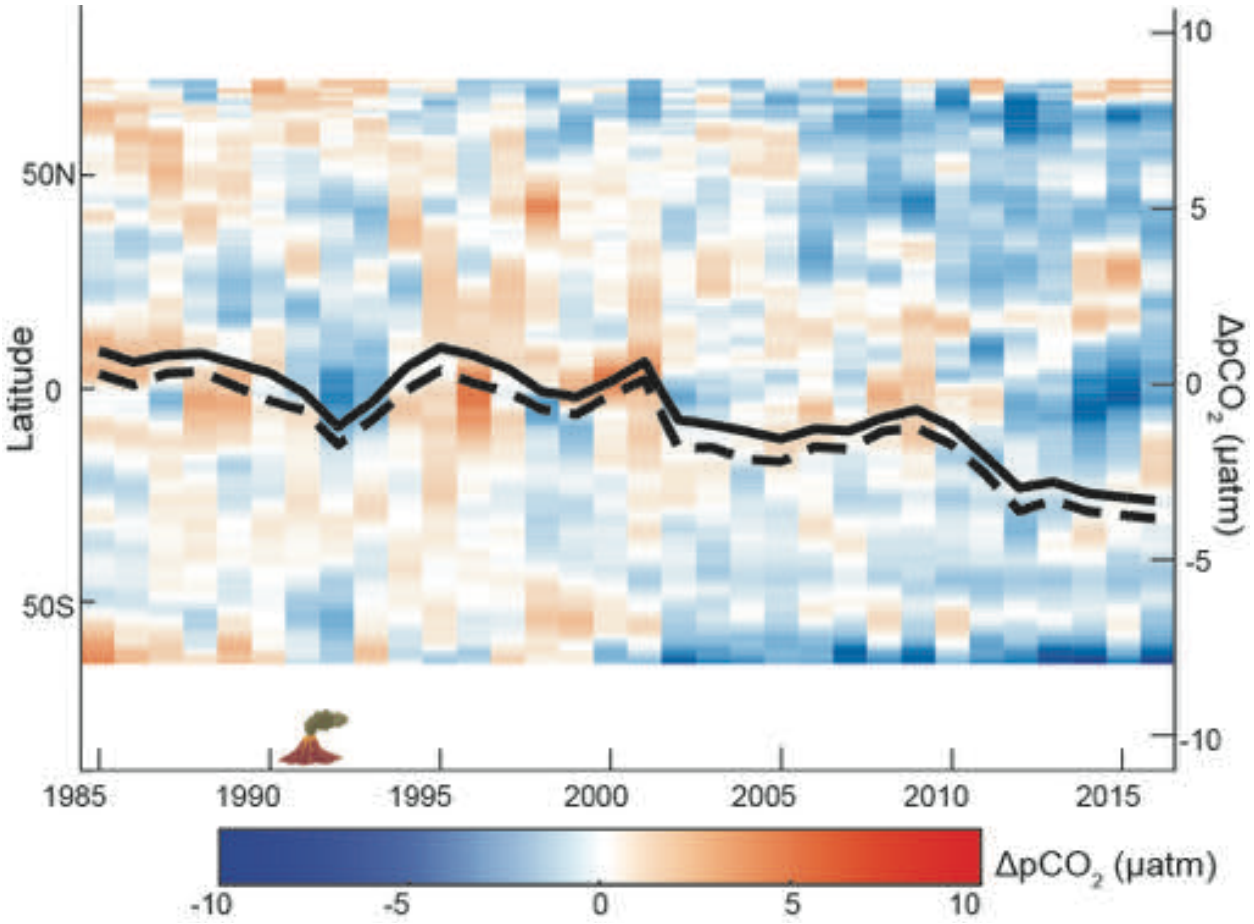

Figure S4: Latitudinal mean anomaly ΔpCO_2 (μatm) from the ensemble mean of the hindcast models. Anomaly is calculated from the 1990-1999 mean. Latitudes with >50% mean ice coverage omitted. Annual ΔpCO_2 time series overlaid in black for global (solid) and global excluding east equatorial Pacific biome (dashed).

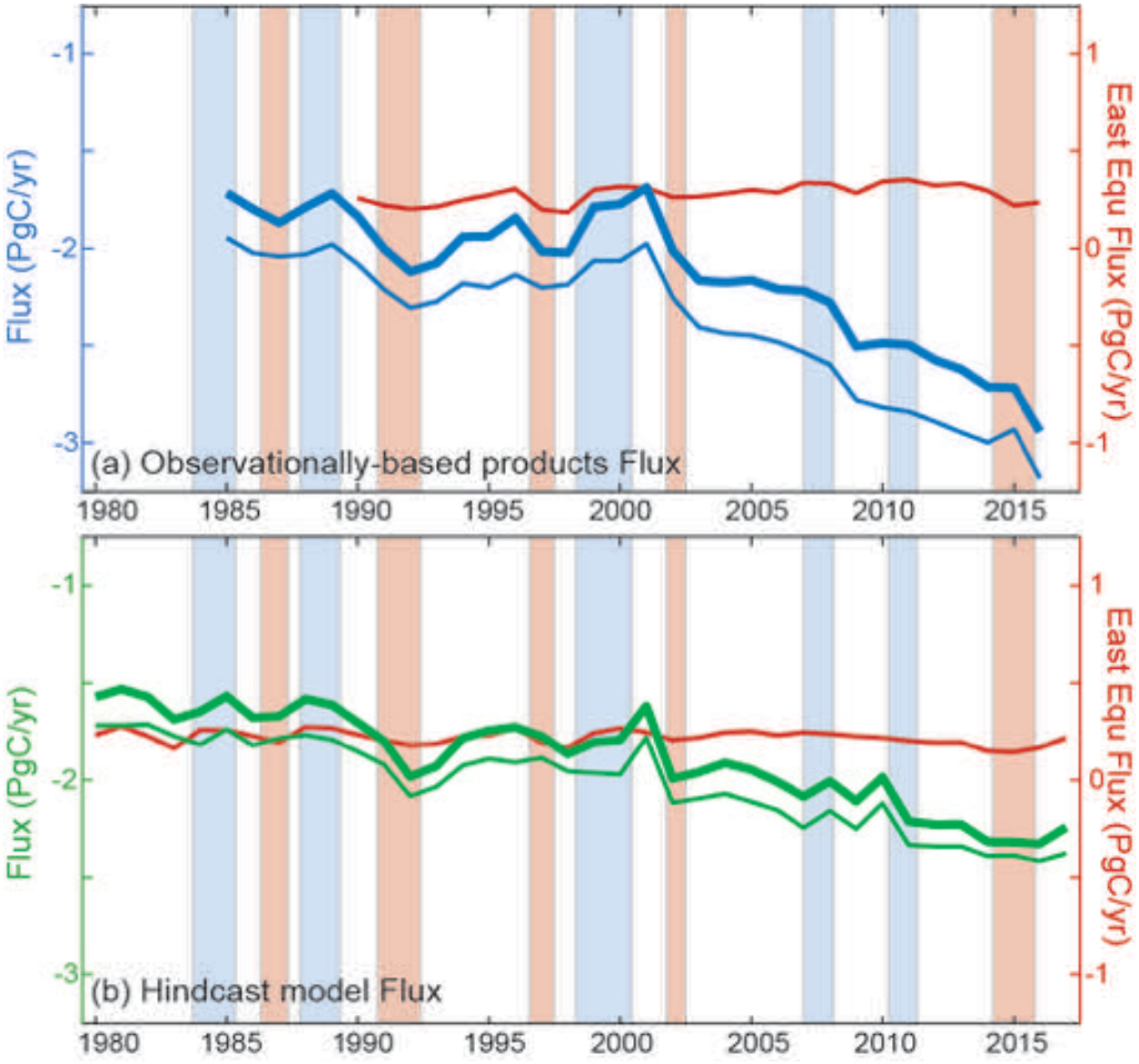

Figure S5: Comparison of global fluxes and fluxes for the globe without the eastern equatorial Pacific (Fay & McKinley 2014). (A) Observationally-based products (blue), (B) hindcast models (green) for global (thick line), global without eastern equatorial Pacific biome (thin line), and only east equatorial Pacific biome (red line). Shaded bars represent ENSO events; blue for La Niña, red for El Niño. Though there is a high inverse correlation between CO_2 fluxes and the Nino 3.4 index in the eastern equatorial Pacific (r = -0.72 for products and r = -0.63 for models), this region is small (4% of the global ocean area) and is not dominant to the global decadal flux variability. Observationally-based product fluxes include 0.45PgC/yr riverine efflux correction.

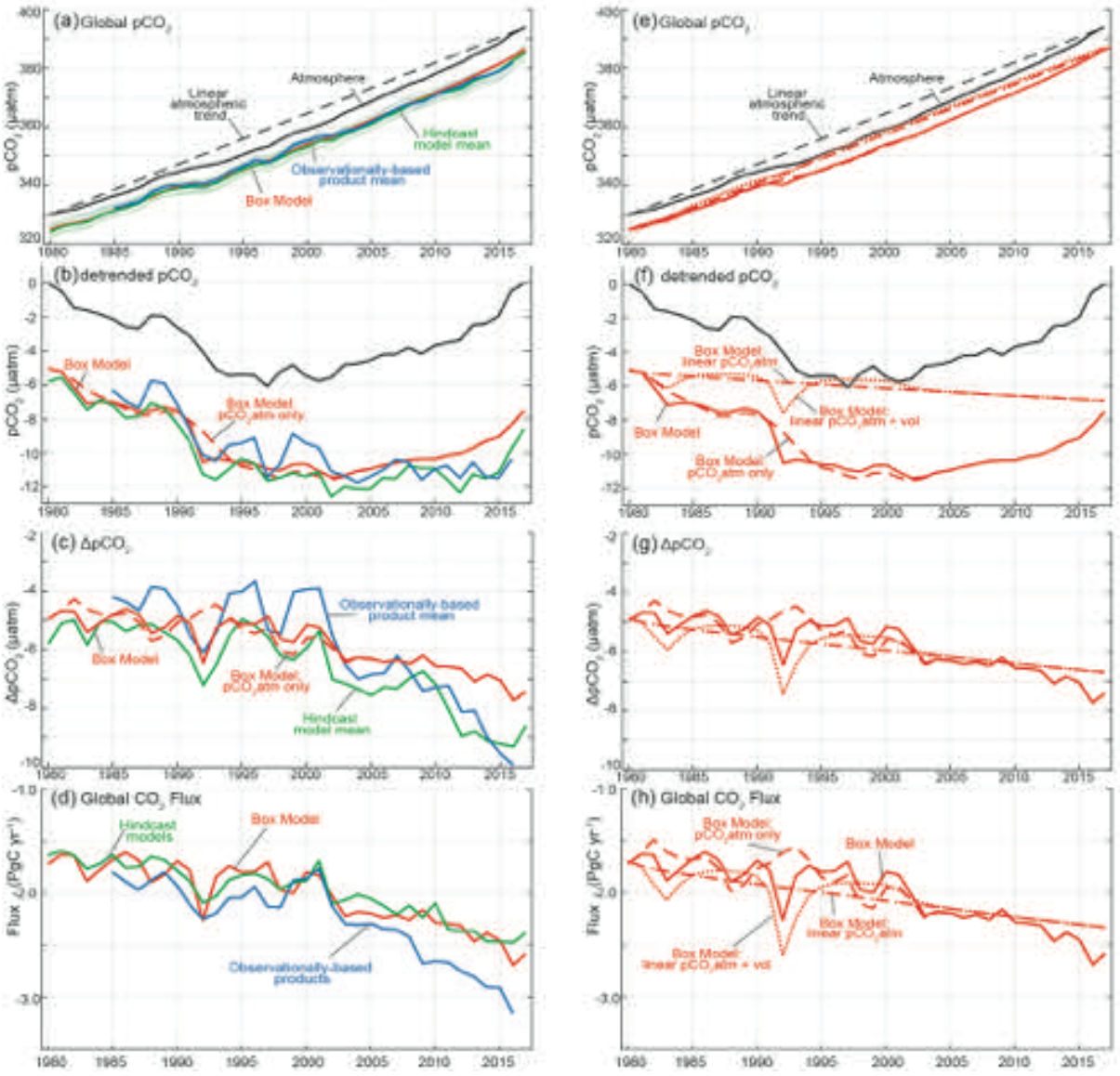

Figure S6: Trends of $pCO_2^{atmosphere}$, pCO_2^{ocean}, and Air-sea CO_2 flux (**A**) with trend, (**B**) detrended with the long-change in $pCO_2^{atmosphere}$ (1.70 µatm/yr from 1980 to 2017), (**C**) ΔpCO_2 (= pCO_2^{ocean} - $pCO_2^{atmosphere}$), and (**D**) global flux (as in Figure 1a). Observationally-based products (blue), hindcast models (green), upper ocean diagnostic box model (red). Hindcast models without the water vapor correction applied to their atmospheric pCO_2 time series are corrected to account for that difference. (**E**) Box model, 4 versions with trend, (**F**) detrended with the long-term $pCO_2^{atmosphere}$ change (1.70 µatm/yr), (**G**) ΔpCO_2 (= pCO_2^{ocean} - $pCO_2^{atmosphere}$), and (**H**) global flux. E-H, the box model forced only with the linear $pCO_2^{atmosphere}$ trend (dot-dash); with both linear $pCO_2^{atmosphere}$ trend and volcano SST (dotted); with observed $pCO_2^{atmosphere}$ only (dash); and with observed $pCO_2^{atmosphere}$ and volcano SST (solid).